Switching Excitation Controller for Enhancement of Transient Stability of Multi-machine Power Systems

Haotian Kang, Yang Liu, Q. H. Wu, *Fellow, IEEE*, and Xiaoxin Zhou, *Fellow, CSEE*, *Fellow, IEEE*

***Abstract*—This paper proposes a switching structure excitation controller (SSEC) to enhance the transient stability of multi-machine power systems. The SSEC switches between a bang-bang funnel excitation controller (BFEC) and a conventional excitation controller (CEC), based on an appropriately designed state-dependent switching strategy. Only the tracking error of rotor angle is required to realize the BFEC in a bang-bang manner with two control values. If the feasibility assumptions of the BFEC are satisfied, the tracking error of rotor angle can be regulated within the predefined error funnels. The power system having the SSEC installed can achieve faster convergence performance compared to that having the CEC implemented only. Simulation studies are carried out in the New England 10-generator 39-bus power system. The control performance of the SSEC is evaluated in the cases that three-phase-to-ground fault and transmission line outage occur in the power system, respectively.**

***Index Terms*—Bang-bang control, multi-machine power systems, switching controller, transient stability.**

I. INTRODUCTION

TRANSIENT stability has always been the key issue of the operation of modern power systems. Stability problems caused by voltage collapse, islanding, faults, lightning strokes and equipment failure, may lead to enormous loss of social economy [1]. Thus high-performance stabilizing controllers are needed to mitigate the consequences of such events. Normally, the excitation control of synchronous generator is considered as the most effective way to improve the transient stability of multi-machine power systems [2].

In practice, the linearized model based controllers are widely used to maintain the stability of power systems, such as the PID excitation controller [3], linear optimal excitation controller [4] and linear adaptive excitation controller [5]. They are capable of improving transient stability of power systems. These methods are based on the linearized model of the power system operating around a specific operation point. However, as for severe external disturbances, faults, changing of network topology, which may drive the system operation point far from the pre-fault equilibrium point, the linear controllers will lose the advantage of damping the severe oscillations [6]. They can hardly provide reliable control performance. Therefore, more attention should be paid on the design of nonlinear excitation controllers.

In recent years, the application of advanced nonlinear excitation control methods proposed for improving the transient stability have received much attention, such as feedback linearization control (FLC) [7], adaptive control [8], and robust control [9]. The FLC is widely used for excitation control of power systems in [2], [7] and [10]. The basic idea of the FLC is to transform a nonlinear system into its (fully or partially) linear representation first. Then the output feedback controller is designed based upon the linear control techniques to enhance the stability of the whole system. Moreover, the optimization of H_2 and H_∞ norm are used for robust excitation controller design to ensure the robustness of the designed controllers. Furthermore, the observer based control method [11], fuzzy-logic damping control techniques [12], [13] and Lyapunov theory [14] are applied to designing the adaptive excitation controller of synchronous generators. Although the above control techniques have been widely used in the excitation control design of power systems, they still have some drawbacks. On one hand, the design of these controllers more or less relies on the accurate model of power systems and thus it is difficult to cope with the parameter uncertainty or external disturbances of power systems. On the other hand, the nonlinear controllers always involve complex control laws, for what they can not be implemented easily in practice.

In this paper, a novel nonlinear SSEC is designed to enhance the transient stability of multi-machine power systems, which switches between a BFEC and a CEC. The BFEC is designed as a bang-bang funnel controller, which was proposed in [15], [16]. The BFEC only requires the knowledge of the relative degree and output variable of the system, and its control signal is bang-bang with two control values. The key objective of the SSEC is to damp out the oscillations of the power system in the cases that severe disturbances occur. In the case that a large disturbance occurs in the power system, the BFEC is switched on first to drive the operation point of the power system into predefined error funnels. Thereafter, a CEC is switched on referring to the switching strategy of the SSEC. Due to the fact that BFEC has damped out the disturbance, the CEC may achieve a better performance around the original operation point. The advantages of the proposed SSEC can be summarized as follows. First of all, only two control values are used by the BFEC to realize its control performance. This characteristic makes the structure of the BFEC simple and it can be easily applied in the real system digitally. Second, we do not need much knowledge of system structure in the bang-

Manuscript received July 3, 2015; revised July 28, 2015; accepted August 30, 2015. Date of publication September 30, 2015; date of current version September 20, 2015. This work was funded by State Key Program of National Natural Science of China (NO. 51437006), and Guangdong Innovative Research Team Program (NO. 201001N0104744201), China.

H. T. Kang, Y. Liu and Q. H. Wu are with the School of Electric Power Engineering, South China University of Technology, Guangzhou 510640, China (Corresponding author: Q. H. Wu, e-mail: wuqh@scut.edu.cn).

X. X. Zhou is with China Electric Power Research Institute, State Grid Corporation of China, Qinghe, Beijing 100192, China.

Digital Object Identifier 10.17775/CSEEJPES.2015.00039

bang controller design process on condition that the feasibility assumptions are satisfied. Third, all the calculation of the bang-bang controller is logical, which decreases the calculation time and complexity of the BFEC in comparison to the continuous controller involving complex differential equations. Fourth, the usage of error funnels and the maximal possible control values enables fast transient response and robust tracking ability of the BFEC.

Overall, this paper is organized as follows. In the first place, the model of the multi-machine power system is presented in Section II, in which the decoupled subsystems are obtained through fully linearization of the multi-machine model. Moreover, the SSEC is designed in Section III. The BFEC and switching strategy are introduced therein. Furthermore, simulation studies are carried out in the IEEE 10-generator 39-bus power system in Section IV. Then the conclusion is illustrated in Section V.

II. Power System Modeling

The third-order simplified model of synchronous generators is used in this paper. The i^{th} generator of the multi-machine power system with n synchronous generators is described as follows [4]:

$$\begin{cases} \dot{\delta}_i = \omega_i - \omega_{0i} \\ \dot{\omega}_i = -\frac{D_i}{2H_i}(\omega_i - \omega_{0i}) + \frac{\omega_{0i}}{2H}(P_{\mathrm{m}i} - P_{\mathrm{e}i}) \\ \dot{E}'_{\mathrm{q}i} = \frac{1}{T'_{\mathrm{d}0i}}(E_{\mathrm{f}i} - E_{\mathrm{q}i}) \end{cases} \tag{1}$$

where $i = 1, 2, \ldots, n$, δ_i is the relative rotor angle, ω_i is the rotor speed, H_i is the inertia constant, $P_{\mathrm{m}i}$ is the mechanical power input, D_i is the damping constant, and $P_{\mathrm{e}i}$ is the active power, $E'_{\mathrm{q}i}$ is the quadrature-axis transient voltage, $E_{\mathrm{q}i}$ is the quadrature-axis voltage, $T'_{\mathrm{d}0i}$ denotes the direct-axis open-circuit transient time constant, $E_{\mathrm{f}i}$ denotes the excitation voltage [9], [11].

$E_{\mathrm{q}i}$, $P_{\mathrm{e}i}$, $Q_{\mathrm{e}i}$, $I_{\mathrm{d}i}$, $I_{\mathrm{q}i}$ and $V_{\mathrm{t}i}$ of i^{th} synchronous generator are shown as follows:

$$\begin{cases} E_{\mathrm{q}i} = E'_{\mathrm{q}i} - (x_{\mathrm{d}i} - x'_{\mathrm{d}i})I_{\mathrm{d}i} \\ P_{\mathrm{e}i} = E'^2_{\mathrm{q}i}G_{ii} + E'_{\mathrm{q}i}\sum_{j=1, j\neq i}^{n} E'_{\mathrm{q}j}B_{ij}\sin\delta_{ij} \\ Q_{\mathrm{e}i} = -E'^2_{\mathrm{q}i}G_{ii} - E'_{\mathrm{q}i}\sum_{j=1, j\neq i}^{n} E'_{\mathrm{q}j}B_{ij}\cos\delta_{ij} \\ I_{\mathrm{d}i} = -E'_{\mathrm{q}i}G_{ii} - \sum_{j=1, j\neq i}^{n} E'_{\mathrm{q}j}B_{ij}\cos\delta_{ij} \\ I_{\mathrm{q}i} = E'_{\mathrm{q}i}G_{ii} + \sum_{j=1, j\neq i}^{n} E'_{\mathrm{q}j}B_{ij}\sin\delta_{ij} \end{cases} \tag{2}$$

where $x_{\mathrm{d}i}$ is the direct-axis reactance, $x'_{\mathrm{d}i}$ is the direct-axis transient reactance, G_{ii} and B_{ii} are the self-conductance and self-susceptance of i^{th} bus respectively, G_{ij} and B_{ij} are the conductance and susceptance of the line between i^{th} and j^{th} bus respectively, $\delta_{ij} = \delta_i - \delta_j$ is the rotor angle deviation between i^{th} and j^{th} bus, $I_{\mathrm{d}i}$ and $I_{\mathrm{q}i}$ are direct- and quadrature-axis currents respectively, $Q_{\mathrm{e}i}$ is the reactive power [9], [11].

Substituting (2) into (1) and we have:

$$\begin{aligned} \dot{\delta}_i =& \omega_i - \omega_{0i} \\ \dot{\omega}_i =& -\frac{D_i}{2H_i}(\omega_i - \omega_{0i}) + \frac{\omega_{0i}}{2H}P_{\mathrm{m}i} \\ & - \frac{\omega_{0i}}{2H}(E'^2_{\mathrm{q}i}G_{ii} + E'_{\mathrm{q}i}\sum_{j=1}^{n} E'_{\mathrm{q}j}B_{ij}\sin\delta_{ij}) \\ \dot{E}'_{\mathrm{q}i} =& -\frac{1 + (x_{\mathrm{d}i} - x'_{\mathrm{d}i}B_{ii})}{T_{\mathrm{d}oi}}E'_{\mathrm{q}i} \\ & + \frac{x_{\mathrm{d}i} - x'_{\mathrm{d}i}}{T_{\mathrm{d}oi}}\sum_{j=1}^{n} E'_{\mathrm{q}j}B_{ij}\cos\delta_{ij} + \frac{1}{T'_{\mathrm{d}0i}}E_{\mathrm{f}i}. \end{aligned} \tag{3}$$

The exact linearization of the multi-machine model method [1] is employed in the following subsection to transform (3) into *Byrnes-Isidori* normal form [17], which is the basic assumption for the design of the BFEC.

A. Exact Linearization of Multi-machine Power System

First of all, the multi-machine power system model will be written in the MIMO general form. The rotor angle deviation $\Delta\delta_i = \delta_i - \delta_{i0}$ is chosen as the output, and the excitation voltage $E_{\mathrm{f}i}$ is chosen as the input. The state variables are defined as $\boldsymbol{x} = [\boldsymbol{x}_1^\top, \ldots, \boldsymbol{x}_i^\top, \ldots, \boldsymbol{x}_n^\top]^\top$, $\boldsymbol{x}_i = [x_{i1}, x_{i2}, x_{i3}]^\top = [\delta_i \quad \omega_i \quad E'_{\mathrm{q}i}]^\top$, the output of i^{th} subsystem is defined as $y_i = x_{i1}$, after that, $u_i = E_{\mathrm{f}i}$ is defined as the input [9], [11]. Then the model of i^{th} synchronous generator can be denoted as

$$\begin{cases} \dot{\boldsymbol{x}}_i = \boldsymbol{f}_i(\boldsymbol{x}_i) + \boldsymbol{g}_i(\boldsymbol{x}_i)u_i \\ y_i = h_i(\boldsymbol{x}_i) \end{cases} \quad i = 1, 2, \ldots, n, \tag{4}$$

where

$$\begin{aligned} \boldsymbol{f}_i(\boldsymbol{x}_i) &= \begin{bmatrix} x_{i2} - \omega_{0i} \\ \frac{D_i}{2H_i}(x_{i2} - \omega_{0i}) + \frac{\omega_{0i}}{2H_i}(P_{\mathrm{m}i} - P_{\mathrm{e}i}) \\ -\frac{1}{T'_{\mathrm{d}0i}}[x_{i3} - (x_{\mathrm{d}i} - x'_{\mathrm{d}i})I_{\mathrm{d}i}] \end{bmatrix}, \\ \boldsymbol{g}_i(\boldsymbol{x}_i) &= \begin{bmatrix} 0 & 0 & \frac{1}{T'_{\mathrm{d}0i}} \end{bmatrix}^\top, \\ h_i(\boldsymbol{x}_i) &= x_{i1} - \delta_{i0}. \end{aligned}$$

Then the general form of a multi-machine power system model can be written as

$$\begin{cases} \dot{\boldsymbol{x}} = \boldsymbol{f}(\boldsymbol{x}) + \boldsymbol{g}(\boldsymbol{x})\boldsymbol{u} \\ \boldsymbol{y} = \boldsymbol{h}(\boldsymbol{x}) \end{cases}, \tag{5}$$

where

$$\begin{aligned} \boldsymbol{f}(\boldsymbol{x}) &= [\boldsymbol{f}_1^\top(\boldsymbol{x}), \boldsymbol{f}_2^\top(\boldsymbol{x}), \ldots, \boldsymbol{f}_n^\top(\boldsymbol{x})]^\top, \\ \boldsymbol{g}(\boldsymbol{x}) &= \begin{bmatrix} \boldsymbol{g}_1(\boldsymbol{x}) & & & \\ & \boldsymbol{g}_2(\boldsymbol{x}) & & \\ & & \ddots & \\ & & & \boldsymbol{g}_n(\boldsymbol{x}) \end{bmatrix} \\ \boldsymbol{h}(\boldsymbol{x}) &= [\boldsymbol{h}_1(\boldsymbol{x}), \boldsymbol{h}_2(\boldsymbol{x}), \ldots, \boldsymbol{h}_n(\boldsymbol{x})]^\top. \end{aligned}$$

A nonlinear coordinate transformation [17] is introduced as: $\boldsymbol{z} = [z_{11}, z_{12}, \ldots, z_{1r_1}, \ldots, z_{i1}, z_{i2}, \ldots, z_{ir_i}, \ldots, z_{nr_n}]^\top = \boldsymbol{\phi}(\boldsymbol{x}) = [h_1(\boldsymbol{x}), \mathcal{L}_f h_1(\boldsymbol{x}), \ldots, \mathcal{L}_f^{r_1-1}h_1(\boldsymbol{x}), \ldots, h_i(\boldsymbol{x}), \mathcal{L}_f h_i(\boldsymbol{x}), \ldots, \mathcal{L}_f^{r_i-1}h_i(\boldsymbol{x}), \ldots, h_n(\boldsymbol{x}), \mathcal{L}_f h_n(\boldsymbol{x}), \ldots, \mathcal{L}_f^{r_n-1}h_n(\boldsymbol{x})]^\top$, where r_i is the relative degree of i^{th} generator model, and the approach to calculate the r_i is presented in [18]. Thus we have

$$\begin{aligned}
&\mathcal{L}_g h_i(\boldsymbol{x}_i) = 0\\
&\mathcal{L}_g\mathcal{L}_f^1 h(\boldsymbol{x}_i) = \mathcal{L}_g(x_{i2}-\omega_{0i}) = 0\\
&\mathcal{L}_f^2 h_i(\boldsymbol{x}_i) = \frac{D_i}{2H_i}(x_{i1}-\omega_{0i}) + \frac{\omega_{0i}}{2H_i}(P_{\mathrm{m}i}-P_{\mathrm{e}i})\\
&\mathcal{L}_g\mathcal{L}_f^2 h_i(\boldsymbol{x}_i) = \frac{\partial(\mathcal{L}_f^2 h_i(\boldsymbol{x}_i))}{\partial \boldsymbol{x}_i}\boldsymbol{g}(\boldsymbol{x}) \neq 0.
\end{aligned}$$

Therefore, the relative degree r_i of i^{th} subsystem is 3. That is to say, the system is fully linearizable. The obtained linearized system model can be written as

$$\begin{cases}\dot{z}_{i1} = z_{i2}\\ \dot{z}_{i2} = z_{i3}\\ \dot{z}_{i3} = \alpha_i(\boldsymbol{z}) + \sum_{j=1}^n \beta_{ij}(\boldsymbol{z})u_j\\ y_i = z_{i1}.\end{cases} \quad i=1,2,\ldots,n. \tag{6}$$

where

$$\begin{aligned}
&\alpha_i(\boldsymbol{z}) = (\mathcal{L}_f^3 h_i(x))|_{\boldsymbol{x}=\boldsymbol{\phi}(\boldsymbol{x})^{-1}(\boldsymbol{z})}\\
&\mathcal{L}_f^3 h_i(\boldsymbol{x}) = \sum_{j=1}^n\left[\frac{\partial\dot{\omega}_i}{\partial x_{j1}}f_{j1}(\boldsymbol{x}) + \frac{\partial\dot{\omega}_i}{\partial x_{j2}}f_{j2}(\boldsymbol{x}) + \frac{\partial\dot{\omega}_i}{\partial x_{j3}}f_{j3}(\boldsymbol{x})\right]\\
&= -\frac{\omega_0}{2H_i}\sum_{j=1}^n\left[\frac{\partial P_{\mathrm{e}i}}{\partial x_{j1}}f_{j1}(\boldsymbol{x}) + \frac{\partial P_{\mathrm{e}i}}{\partial x_{j3}}f_{j3}(\boldsymbol{z})\right] - \frac{D_i}{2H_i}f_{i2}(\boldsymbol{x})\\
&\beta_{ij}(\boldsymbol{z}) = (\mathcal{L}_{g_j}\mathcal{L}_f^2 h_i(\boldsymbol{x}))|_{\boldsymbol{x}=\boldsymbol{\phi}(\boldsymbol{x})^{-1}(\boldsymbol{z})}\\
&\mathcal{L}_{g_j}\mathcal{L}_f^2 h_i(\boldsymbol{x}) = \frac{\partial\dot{\omega}_i}{\partial E'_{\mathrm{q}j}}\frac{1}{T_{\mathrm{d}0j}} = \frac{\omega_0}{2H_iT_{\mathrm{d}0j}}\frac{\partial P_{\mathrm{e}i}}{\partial E'_{\mathrm{q}j}}\ (j=1,2,\ldots,n).
\end{aligned}$$

From (1), we can obtain

$$\begin{aligned}
\frac{dP_{\mathrm{e}i}}{dt} &= \sum_{j=1}^n\left(\frac{\partial P_{\mathrm{e}i}}{\partial x_{j3}}f_{j3} + \frac{\partial P_{\mathrm{e}i}}{\partial x_{j1}}f_{j1}\right)\\
&= \sum_{j=1}^n\left(\frac{\partial P_{\mathrm{e}i}}{\partial x_{j3}}f_{j3} + \frac{\partial P_{\mathrm{e}i}}{\partial x_{j1}}f_{j1} + \frac{\partial P_{\mathrm{e}i}}{\partial E'_{\mathrm{q}j}}\frac{1}{T'_{\mathrm{d}0i}}u_j\right).
\end{aligned}$$

From the above, the following equation can be given:

$$\alpha_i = -\frac{\omega_0}{2H_i}\frac{dP_{\mathrm{e}i}}{dt} + \frac{D_i}{2H_i}\dot{\omega}_i - \sum_{j=1}^n\beta_{ij}u_j.$$

Thus the decoupled model of linearized system (6) can be obtained as:

$$\begin{cases}\dot{z}_{i1} = z_{i2}\\ \dot{z}_{i2} = z_{i3}\\ \dot{z}_{i3} = -\dfrac{\omega_0}{2H_i}\dfrac{dP_{\mathrm{e}i}}{dt} + \dfrac{D_i}{2H_i}\dot{\omega}_i\\ y_i = z_{i1}.\end{cases} \quad i=1,2,\ldots,n. \tag{7}$$

Moreover, the active power and its derivative can be denoted as [9], [11]

$$\begin{aligned}
&P_{\mathrm{e}i} = E'_{\mathrm{q}i}I_{\mathrm{q}i} + (x_{\mathrm{q}i}-x'_{\mathrm{d}i})I_{\mathrm{q}i}I_{\mathrm{d}i}\\
&\frac{dP_{\mathrm{e}i}}{dt} = I_{\mathrm{q}i}\frac{dE'_{\mathrm{q}i}}{dt} + E'_{\mathrm{q}i}\frac{dI_{\mathrm{q}i}}{dt} + (x_{\mathrm{q}i}-x'_{\mathrm{d}i})\frac{dI_{\mathrm{q}i}I_{\mathrm{d}i}}{dt}.
\end{aligned} \tag{8}$$

Substituting (8) and the third equation of system (1) into (7), we can obtain:

$$\begin{cases}\dot{z}_{i1} = z_{i2}\\ \dot{z}_{i2} = z_{i3}\\ \dot{z}_{i3} = f_i(\boldsymbol{z}) + b_i(\boldsymbol{z})u_i\\ y_i = z_{i1}.\end{cases} \quad i=1,2,\ldots,n. \tag{9}$$

where

$$\begin{aligned}
f_i(z) &= \frac{-\omega_0}{2H_i}\left[\frac{D_i}{\omega_0}\dot{\omega}_i + E'_{\mathrm{q}i}\dot{I}_{\mathrm{q}i} + (x_{\mathrm{q}i}-\dot{x}_{\mathrm{d}i})\frac{d(I_{\mathrm{d}i}I_{\mathrm{q}i})}{dt}\right]\\
&+ \frac{\omega_0 I_{\mathrm{q}i}}{2H_iT'_{\mathrm{d}0i}}E_{\mathrm{q}i}\\
b_i(z) &= -\frac{\omega_0 I_{\mathrm{q}i}}{2H_iT'_{\mathrm{d}0i}}.
\end{aligned}$$

III. Design of the SSEC

The bang-bang funnel controller proposed in [19] is employed here for the design of BFEC. According to a state-dependent switching strategy, the SSEC switches between the BFEC and the conventional excitation controller.

A. Third-Order Bang-Bang Funnel Controller

Since the multi-machine power system modeled in Section II can be decoupled into n subsystems, and each of them has relative degree of $r=3$. Thus the third-order bang-bang funnel controller is used to realize the excitation control of a synchronous generator. In order to simplify the switching logic, we consider constant funnels, which can also provide reliable performance. According to the results of [19], the bang-bang funnel controller is able to regulate the output tracking error within pre-specified error funnels if the feasibility assumptions presented in [19] are satisfied.

The switching logic $\mathcal{S}$ of the third-order bang-bang funnel controller can be described as

$$\begin{aligned}
&q_1(t) = \mathcal{G}(e(t), \varphi_0^+ - \varepsilon_0^+, \varphi_0^- + \varepsilon_0^-, q_1(t-)),\\
&q_1(0-) = q_1^0 \in \{\mathrm{true}, \mathrm{false}\},\\
&q_2(t) =\\
&\begin{cases}\mathcal{G}(\dot{e}(t), -\lambda_1^- - \varepsilon_1^+, \varphi_1^- + \varepsilon_1^-, q_2(t-)), & \text{if } q_1(t) = \mathrm{true},\\ \mathcal{G}(\dot{e}(t), \varphi_1^+ - \varepsilon_1^+, \lambda_1^+ + \varepsilon_1^-, q_2(t-)), & \text{if } q_1(t) = \mathrm{false},\end{cases}\\
&q_2(0-) = q_2^0 \in \{\mathrm{true}, \mathrm{false}\},\\
&q(t) =\\
&\begin{cases}\mathcal{G}(\ddot{e}(t), -\lambda_2^- - \varepsilon_2^+, \varphi_2^- + \varepsilon_2^-, q(t-)), & \text{if } q_2(t) = \mathrm{true},\\ \mathcal{G}(\ddot{e}(t), \varphi_2^+ - \varepsilon_2^+, \lambda_2^+ + \varepsilon_2^-, q(t-)), & \text{if } q_2(t) = \mathrm{false},\end{cases}\\
&q(0-) = q^0 \in \{\mathrm{true}, \mathrm{false}\}.
\end{aligned} \tag{10}$$

where $\mathcal{G}(e, \overline{e}, \underline{e}, q_{\mathrm{old}}) := [e \geq \overline{e} \vee (e > \underline{e} \wedge q_{\mathrm{old}})]$, $\overline{e}(\cdot)$ is the upper switch trigger [19], $\underline{e}(\cdot)$ is the lower switch trigger [19], $e(\cdot)$ is the system output tracking error, which drives the system [19], and $q_{\mathrm{old}} \in \{\mathrm{true}, \mathrm{false}\}$, $\varphi_i^{\pm}$ are the funnel boundaries used to define funnel $\mathcal{F}_i := \{(t, e^{(i)}(t)) \in \mathbb{R}_{\geq 0} \times \mathbb{R} | \varphi_i^- \leq e^{(i)}(t) \leq \varphi_i^+\}$, $\lambda_i^+, \lambda_i^- \in \mathbb{R}_{\leq 0}$ represent the desired minimal or maximal value of $e^{(i)}(t)$, which aim to increase or decrease the previous order derivative of output tracking error $e^{(i-1)}(t)$ by a certain rate, $\varepsilon_i^+, \varepsilon_i^- \in \mathbb{R}_{\geq 0}$ is designed to trigger a switch in the internal or external signals when the errors get close to the funnel boundaries [19], $q(t-) := \lim_{\varepsilon \searrow 0} q(t-\varepsilon)$ [19]. $q(t)$ is the output of the switching logic. Moreover, the control law of the bang-bang funnel controller can be simply given by [19]

$$u_B(t) = \begin{cases}U^-, & \text{if } q(t) = \mathrm{true},\\ U^+, & \text{if } q(t) = \mathrm{false}.\end{cases} \tag{11}$$

The working mechanism of the third-order bang-bang funnel controller is illustrated in Fig. 1. It can be noticed that the control of the dynamics of $e^{(i)}(t)$ is realized through the control of $e^{(i+1)}(t)(i = 0, 1)$. And $e^{(2)}(t)$ can be directly controlled by the switching of $q(t)$.

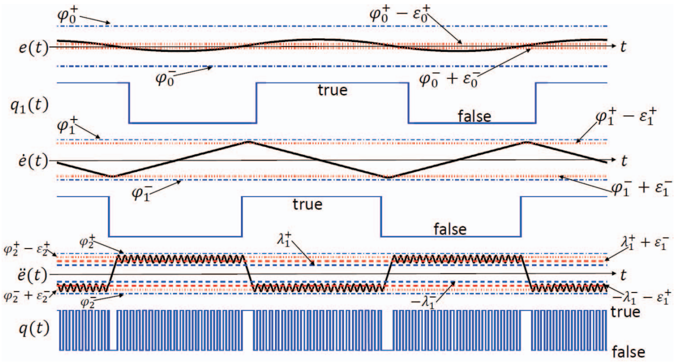

Fig. 1. Working mechanism of the third-order bang-bang funnel controller.

B. Design of BFEC

The BFEC is designed as a bang-bang funnel controller. In term of the feasibility assumptions of BFEC, F_1 has been shown satisfied in (9). As $y_{\text{ref}} = 0$, F_2 can be shown fulfilled. The control law of BFEC can be given as

$$u_B(t) = \begin{cases} E_{\text{f\_min}}, & \text{if } q(t) = \text{true}, \\ E_{\text{f\_max}}, & \text{if } q(t) = \text{false}. \end{cases} \tag{12}$$

C. Introduction of the CEC

The simplified IEEE DC-1A excitation model [20] is described by Fig. 2, in which V_{PSS} is the output of PSS, V_{t} denotes the terminal voltage, and V_{REF} is the reference value of terminal voltage, $\Delta E_{\text{f}} = E_{\text{f}} - E_{\text{f0}}$ is the output of the exciter.

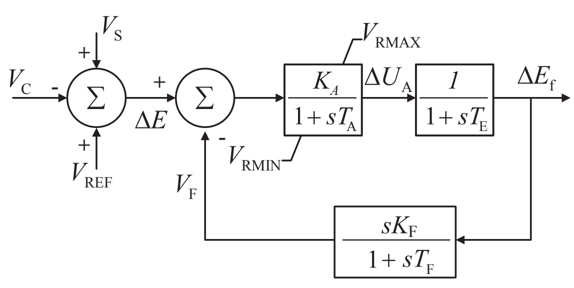

Fig. 2. Simplified type DC-1A exciter.

D. The Switching Strategy

The SSEC switches between the BFEC and the CEC based upon the state-dependent switching strategy. As the rotor angle δ is chosen as the system output, its tracking error can be written as $e = y - y_{\text{ref}} = \Delta\delta$. A boundary $\mathcal{B} := \{(t, e) \in \mathbb{R}_{\geq 0} \times \mathbb{R} | b^-(t) \leq e \leq b^+(t)\}$ is designed as the switching surface of the SSEC. In the "steady state," it has $\Delta\delta = 0$. If tracking error e hits the boundary, the bang-bang controller is switched on to damp the oscillations. Under the control of BFEC, e returns back into the $\mathcal{B}$. Then the CEC is switched on operation. To eliminate the chattering of SSEC on the switching boundary, a time delay Δ_b is introduced in the switching strategy. Then the switching strategy can be given as

$$u(t) = pu_{\text{B}}(t) + (1 - p)u_{\text{C}}(t) \tag{13}$$

where

$$p = \begin{cases} 1, & \text{if } \delta(t) \notin \mathcal{B} \\ 0, & \text{if } \forall t \in [t_0, t_0 + \Delta_b]\, \delta(t) \in \mathcal{B}. \end{cases}$$

If $u(t) = u_{\text{B}}(t)$, the BFEC is switched on. If $u(t) = u_{\text{C}}(t)$, the CEC is switched on.

E. Parameters of SSEC

Parameters of the BFEC designed for the power system (1) are given as follows:

$$\begin{aligned} \varphi_0^+ &= -\varphi_0^- \equiv 4, & \varepsilon_0^+ &= \varepsilon_0^- \equiv 3.9, \\ \varphi_1^+ &= -\varphi_1^- \equiv 3, & \varepsilon_1^+ &= \varepsilon_1^- \equiv 2.9, \\ \varphi_2^+ &= -\varphi_2^- \equiv 6, & \varepsilon_2^+ &= \varepsilon_2^- \equiv 0.5, \end{aligned}$$

$$\begin{aligned} \lambda_1^+ &= \lambda_1^- \equiv 0, & & \\ \lambda_2^+ &= \lambda_2^- \equiv 4.5, & U^+ &= -U^- = 1 \\ \lambda_3^+ &= \lambda_3^- \equiv 25, & & \end{aligned}$$

and the switching surface is given as $\mathcal{B} := \{(t, e) \in \mathbb{R}_{\geq 0} \times \mathbb{R} | -1.5 \leq e \leq 1.5\}$.

IV. Control Performance Evaluation and Comparison

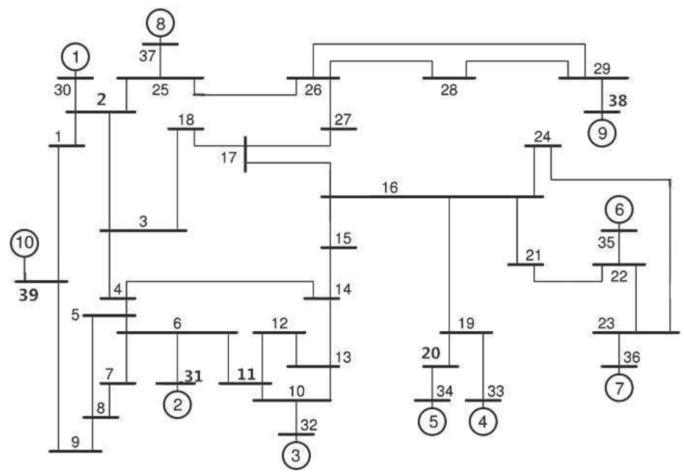

Fig. 3. New England 10-generater 39-bus power system.

The New England 10-generator 39-bus power system shown in Fig. 3 is used as the test system to evaluate the performance of the proposed controller, and the parameters of the system are given in [21]. Synchronous generators are simulated with their third-order models. Generator 1 is installed with the SSEC. Other synchronous generators of the power system are controlled by the simplified IEEE DC-1A exciter and a PSS.

Two cases, three-phase-to-ground fault and transmission line outage occurs in the power system respectively, are studied in this section. The two accidents both lead to severe disturbances of the power system. The performance of generator 1 having SSEC installed is evaluated by its comparing with the generator 1 having CEC installed. The rotor angle, rotor speed, active power, and terminal voltage of generator 1 and generator 6 are illustrated respectively for comparison. With respect to the CEC, its parameters are chosen as: $K_{\mathrm{A}} = 400$, $T_{\mathrm{A}} = 0.05$, $K_{\mathrm{F}} = 0.025$, $T_{\mathrm{F}} = 1$, $T_{\mathrm{E}} = 0.095$.

A. A Three-Phase-to-Ground Fault on the Transmission Line Between Bus-1 and Bus-2

In this case, a three-phase-to-ground fault occurs on the transmission line between buses 1 and 2 from t=0.5 s to t=0.6 s. Then the transmission line is cut off by the protection system at t=0.6 s. The fault line is switch on operation at t=1.3 s. With respect to the operation of the SSEC, the BFEC is switched on between t=0.5 s and t=6 s. The CEC is switched on operation during the remaining simulation time.

Fig. 4 presents the rotor angle, rotor speed, active power output and terminal voltage of generator 1. Then the excitation voltage of generator 1 is depicted in Fig. 5. In each figure, the solid line represents the response of the system having the SSEC installed. And the dashed line represents the response of the system having the CEC implemented only. From the presented results, it can be seen that the SSEC responses faster than the CEC. Due to the switching strategy of the SSEC, the BFEC is switched on first to stabilize the system during the initial post-fault stage with two big enough control values within a few oscillation cycles. Then the CEC is switched on to stabilize the power system to its original operation point asymptotically. According to Fig. 4, the rotor angle, rotor speed deviation, active power output and terminal voltage of generator 1 having SSEC installed present less oscillations. Moreover, the excitation voltage of generator 1 illustrated in Fig. 5 reveals that the BFEC is able to respond faster to the fluctuation of rotor angle in comparison to the CEC. Meanwhile, the terminal voltage of generator 1 is stable, and it can be reset to the pre-fault value. The designed controller is logic-based without involving complex calculation. With the bang-bang mechanism applied, the SSEC is able to provide better transient stability control performance than the CEC.

B. Transmission Line Outage Between Bus-1 and Bus-2

Transmission line outage increases line impedance, which will limit the power transfer capability of the power system. And the time used for restoring the transmission line needs to be limited in case of drastic consequences. In this subsection, the transmission line between bus-1 and bus-2 is cut off incorectly by the protection system at t=0.5 s, and the transmission line is switched on operation at t=1.3 s. With respect to the SSEC, the BFEC works from t=0.5 s to t=4 s. The CEC works during the remaining simulation time.

In Fig. 6 and Fig. 7, dynamics of generator 1 having the SSEC implemented and having the CEC installed only is illustrated, respectively. In each figure, the solid line represents the system state response controlled by the SSEC, and the dashed line represents the system state response controlled by the CEC only. According to the simulation results, both the rotor angle and the rotor speed deviations of generator 1 controlled by the SSEC show less oscillation than those of the generator 1 implemented with the CEC only. Due to the improvement of rotor angle and rotor speed dynamics, the active power output and terminal voltage of the generator 1 controlled by the SSEC present less fluctuation. Moreover, less steady-state tracking error can be found in the generator 1 having SSEC installed in comparison with the generator 1 having the CEC implemented. From these simulation results, it can be noticed that the SSEC works much better than the CEC in the case that transmission line outage occurs in the power system.

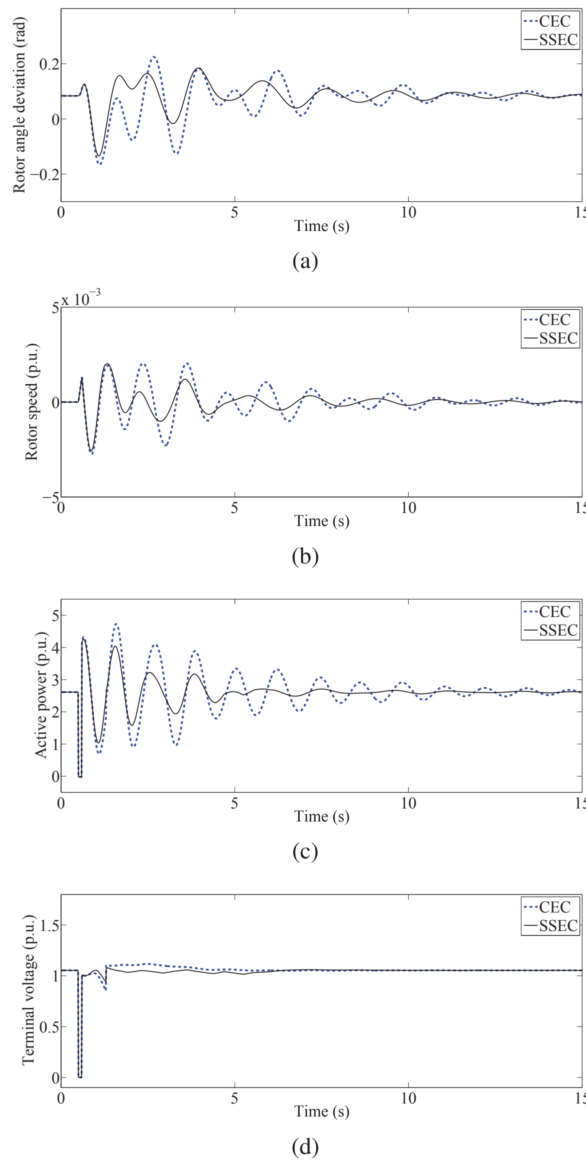

Fig. 4. Dynamics of generator 1 obtained in the case that a three-phase fault occurs in the power system. (a) Rotor angle deviation. (b) Rotor speed. (c) Active power output. (d) Terminal voltage.

The dynamics of generator 6 are presented in Fig. 8. It can

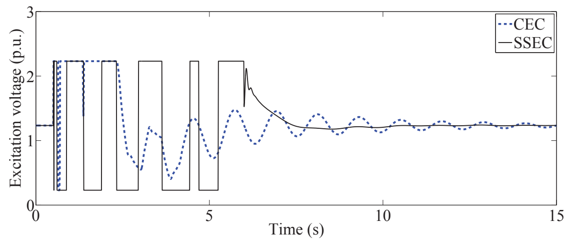

Fig. 5. Excitation voltage of generator 1 obtained in the case that a three-phase fault occurs in the power system.

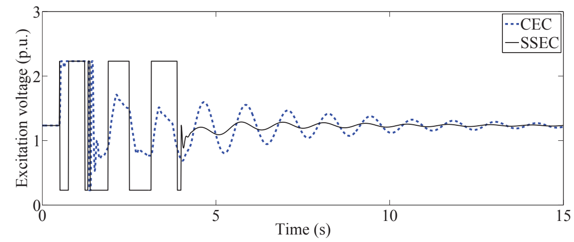

Fig. 7. Excitation voltage of generator 1 obtained in the case that a transmission line outage occurs in the power system.

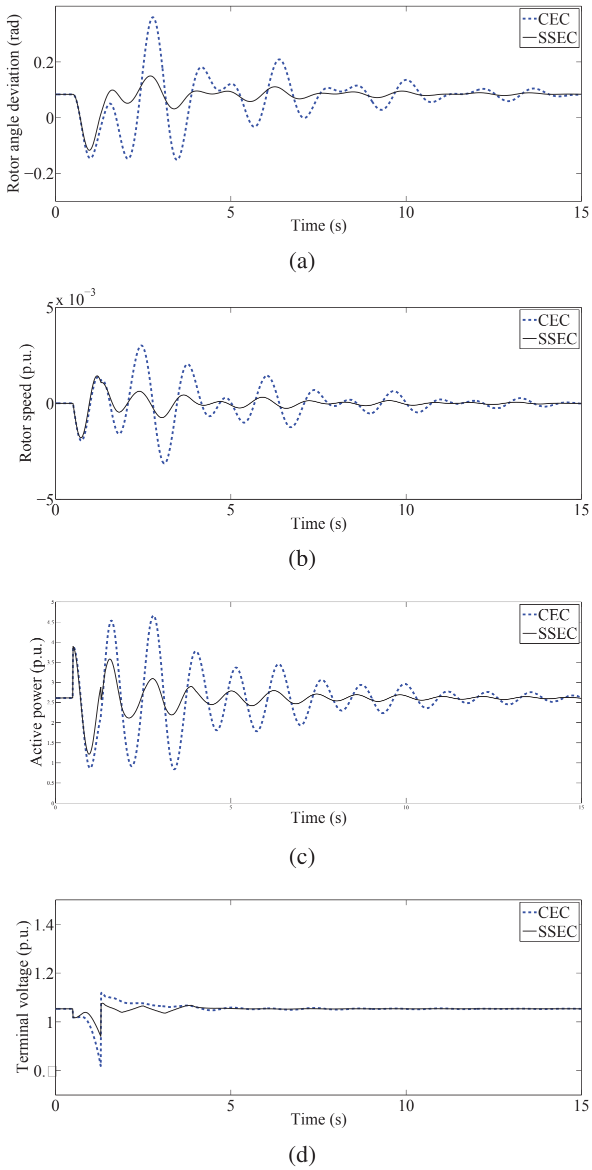

Fig. 6. Dynamics of generator 1 obtained in the case that a transmission line outage occurs in the power system. (a) Rotor angle deviation. (b) Rotor speed. (c) Active power output. (d) Terminal voltage.

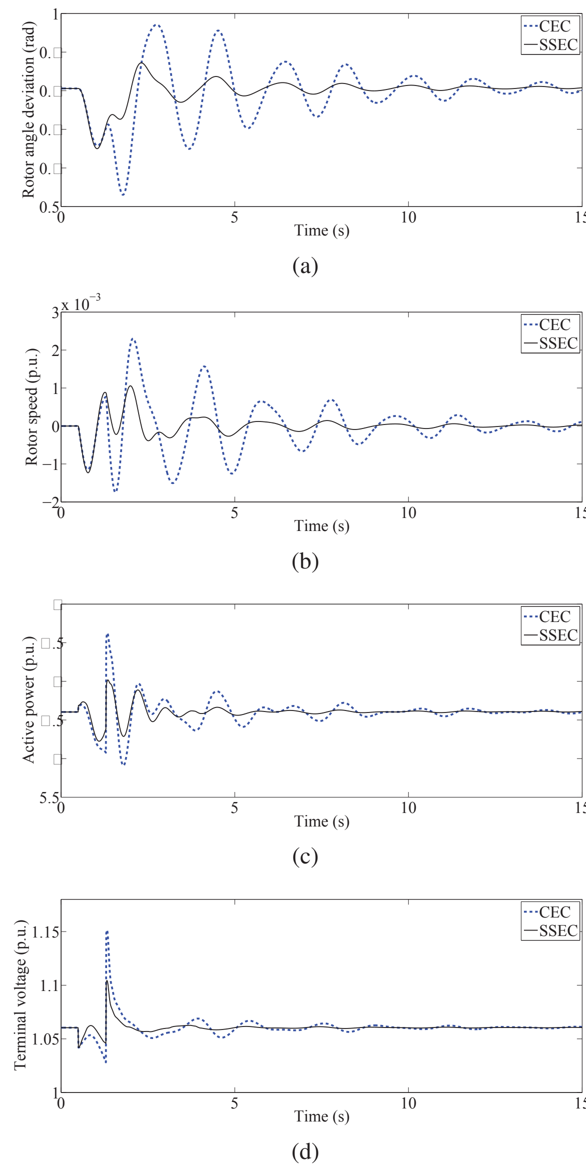

Fig. 8. Dynamics of generator 6 obtained in the case that a transmission line outage occurs in the power system. (a) Rotor angle deviation. (b) Rotor speed. (c) Active power output. (d) Terminal voltage.

be observed that the generator 6 of the power system having the SSEC installed presents less oscillations in rotor angle, rotor speed, active power and terminal voltage than the one of the power system having the CEC equipped. This is due to that the BFEC is capable of damping out the oscillations during the initial post-fault stage. The unbalanced swing energy of the entire power system is reduced and thus other generators of the power system is able to present better transient stability performance as well.

V. Conclusion

This paper has proposed a SSEC to investigate the feasibility of the bang-bang control for improving the transient stability of multi-machine power systems. The SSEC switches between a BFEC and a CEC. The design of the BFEC does not require the accurate system model and only the knowledge of relative degree of the system is needed.

Simulation studies are undertaken in the cases that three-phase-to-ground fault and transmission line outage occur in the system, respectively. The SSEC is capable of enhancing both the rotor angle stability and the voltage stability of the power system. The generator controlled by the SSEC presents faster convergence performance and smaller steady-state tracking errors than the generator controlled by the CEC does. This can be attributed to that the BFEC involves logic operation only and it can provide faster responding speed to the rotor angle oscillations during the initial post-fault stage. The switching action of the BFEC, which offers a maximum control energy, has fully explored the potential of the excitation system of synchronous generators. Thus the BFEC is able to damp out more unbalanced swing energy of the entire power system than the CEC.

Less interactions can be found between the generators of the power system having SSECs installed. The design of the BFEC does not rely on the system parameters. And the local state variable information, rotor speed deviation of a generator, is used in the control loop. Therefore, the SSEC is able to achieve better decoupling of the dynamics between different generators. The coordination between SSECs installed in different generators will be reported in near future.

References

[1] M. A. Mahmud, H. R. Pota, M. Aldeen, and M. J. Hossain, "Partial feedback linearizing excitation controller for multimachine power systems to improve transient stability," *IEEE Transactions on Power Systems*, vol. 29, no. 2, pp. 561–571, March 2014.

[2] B. K. Kumar, S. N. Singh, and S. C. Srivastava, "A decentralized nonlinear feedback controller with prescribed degree of stability for damping power system oscillations," *Electric Power System Research*, vol. 77, no. 3, pp. 204–211, 2007.

[3] A. R. Mahran, B. W. Hogg, and M. L. El-Sayed, "Co-ordinated control of synchronous generator excitation and static var compensator," *IEEE Transactions on Energy Conversion*, vol. 7, no. 4, pp. 615–622, Dec 1992.

[4] P. Kundur, N. J. Balu, and M. G. Lauby, *Power System Stability and Control*, vol. 7. New York: McGraw-Hill, 1994.

[5] Q. H. Wu and B. W. Hogg, "Adaptive controller for a turbogenerator system," *IEE Proceedings-Control Theory and Applications*, vol. 135, no. 1, pp. 35–42, January 1988.

[6] M. J. Hossain, H. R. Pota, V. A. Ugrinovskii, and R. A. Ramos, "Voltage mode stabilisation in power systems with dynamic loads," *International Journal of Electric Power & Energy Systems*, vol. 32, no. 9, pp. 911–920, 2010.

[7] D. Gan, Z. Qu, and H. Cai, "Multi machine power system excitation control design via theories of feedback linearization control and nonlinear robust control," *International Journal of Communications, Network and System Science*, vol. 31, no. 4, pp. 519–527, 2000.

[8] J. C. Deng and X. P. Zhang, "Robust damping control of power systems with TCSC: A multi-model bmi approach with h_2 performance," *IEEE Transactions on Power Systems*, vol. 29, no. 4, pp. 1512–1521, July 2014.

[9] L. Jiang, Q. H. Wu, J. Wang, C. Zhang, and X. X. Zhou, "Robust observer-based nonlinear control of multimachine power systems," *IEE Proceedings-Generation Transmission and Distribution*, vol. 148, no. 6, pp. 623–631, Nov 2001.

[10] A. E. Leon, J. A. Solsona, and M. I. Valla, "Comparison among nonlinear excitation control strategies used for damping power system oscillations," *Energy Conversion Managezine*, vol. 53, no. 1, pp. 55–67, 2012.

[11] L. Jiang, Q. H. Wu, and J. Y. Wen, "Decentralized nonlinear adaptive control for multimachine power systems via high-gain perturbation observer," *IEEE Transactions on Circuits and Systems-I*, vol. 51, no. 10, pp. 2052–2059, Oct 2004.

[12] D. Z. Fang, Y. Xiaodong, T. S. Chung, and K. P. Wong, "Adaptive fuzzy-logic svc damping controller using strategy of oscillation energy descent," *IEEE Transactions on Power Systems*, vol. 19, no. 3, pp. 1414–1421, Aug 2004.

[13] E. Handschin, W. Hoffmann, F. Reyer, T. Stephanblome, U. Schlucking, D. Westermann, and S. S. Ahmed, "A new method of excitation control based on fuzzy set theory," *IEEE Transactions on Power Systems*, vol. 9, no. 1, pp. 533–539, Feb 1994.

[14] H. Liu, Z. Hu, and Y. Song, "Lyapunov-based decentralized excitation control for global asymptotic stability and voltage regulation of multi-machine power systems," *IEEE Transactions on Power Systems*, vol. 27, no. 4, pp. 2262–2270, Nov 2012.

[15] C. M. Hackl, N. Hopfe, A. Ilchmann, M. Mueller, and S. Trenn, "Funnel control for systems with relative degree two," *SIAM Journal on Control and Optimization*, vol. 51, no. 2, pp. 965–995, 2013.

[16] T. Singh and S. Vadali, "Robust time-optimal control-frequency domain approach," *Journal of Guidance Control and Dynamics*, vol. 17, no. 2, pp. 346–353, 1994.

[17] A. Isidori, *Nonlinear Control Systems*, vol. 1. London: Springer, 1995.

[18] Q. Lu, Y. Sun, and S. Mei, *Nonlinear Control Systems and Power System Dynamics*, vol. 10. US: Springer, 2001.

[19] D. Liberzon and S. Trenn, "The bang-bang funnel controller for uncertain nonlinear systems with arbitrary relative degree," *IEEE Transactions on Automatic Control*, vol. 58, no. 12, pp. 3126–3141, Dec 2013.

[20] *IEEE Recommended Practice for Excitation System Models for Power System Stability Studies*, IEEE Standard 421.5-2005 (Revision of IEEE Standard 421.5-1992), 2006.

[21] M. A. Pai, *Energy Function Analysis for Power System Stability*. Verlag US: Springer, 1989.

Haotian Kang obtained a B.Sc degree in Mathematics and applied mathematics from South China University of Technology (SCUT), Guangzhou, China. He is currently pursing the M.Sc degree in electrical engineering in SCUT. His research interest is concerned within the area of power system stability control.

Yang Liu obtained a B.E. degree in electrical engineering from South China University of Technology (SCUT), Guangzhou, China, in 2012. He is currently pursing the Ph.D degree at the same area in SCUT. His research interests include the area of power system stability control and power quality evaluation.

Qinghua Wu (M'91, SM'97, F'11) obtained a Ph.D. degree in electrical engineering from The Queens University of Belfast (QUB), U.K. in 1987. He worked as a Research Fellow and subsequently a Senior Research Fellow in QUB from 1987 to 1991. He joined the Department of Mathematical Sciences, Loughborough University, U.K. in 1991, as a Lecturer, subsequently he was appointed Senior Lecturer. In 1995, he joined The University of Liverpool, U.K. to take up the Chair of Electrical Engineering in the Department of Electrical Engineering and Electronics. Now he is with the School of Electric Power Engineering, South China University of Technology, China, as a Distinguished Professor and the Director of Energy Research Institute of the University. Professor Wu has published more than 440 technical publications, including 220 journal papers, 20 book chapters and 3 research monographs published by Springer. He is a Fellow of IEEE, Fellow of IET, Chartered Engineer and Fellow of InstMC. His research interests include nonlinear adaptive control, mathematical morphology, evolutionary computation, power quality and power system control and operation. He has received a National Semiconductor Advanced Technology Award, National Semiconductor Corporation, USA; Remuneration Award to an exceptional merit and performance, Science and Engineering Research Council, UK; Donald Julius Groen Prize for the best paper published in Journal of Systems and Control Engineering. His research interests include nonlinear adaptive control, mathematical morphology, evolutionary computation, power quality and power system control and operation.

Xiaoxin Zhou (F'95) graduated from Tsinghua University, China, in 1965. He is a member of Chinese Academy of Sciences (CAS), a Fellow of IEEE and Academician of Chinese Academy of Sciences. Currently he also serves as the Honorary President of China Electric Power Research Institute (CEPRI), Executive Director of China Society of Electrical Engineering (CSEE), Director of the Study Committee, and the Executive Director of China Electrotechnical Society (CES).

Professor Zhou has devoted himself to research on power system analysis and computation methods for decades. He has led his research group and successfully developed the Power System Analysis Software Package (PSASP), the first large-sale power system analysis software in China, which has been widely applied in the Chinese power utilities. Since the 1990s, he has committed to research on power electronics, digital simulation technology, and power system security and stability monitoring and control theory. Additionally, he has managed a national basic research program, "Research on the fundamental theory of improving operation reliability of the large-scale interconnected power systems," as the chief scientist. Professor Zhou won the top-grade national science and technology progress award for three times in 1985, 2008 and 2009, respectively. He also won the IEEE PES Nari Hingorani FACTS Award in 2008 and the Prize of Ho Leung Ho Lee Foundation for Scientific and Technological Progress in 2009. His main research interests include power system analysis and control, power system digital simulation, flexible AC transmission system (FACTS).